Journal of Geographic Information and Decision Analysis, vol. 2, no. 2, pp. 168 - 181, 1998

Estimating Daily Regional Rainfall Fields by Multiquadric Functions: Accuracy of Interpolation and Decision Making

Annegret H. Thieken
Institute of Geological Sciences, Section of Environmental Geology, Martin-Luther-University, Halle-Wittenberg, Domstrasse 5, D-06108 Halle (Saale), Germany
thieken@geologie.uni-halle.de

ABSTRACT **This paper reports on multiquadric functions', a specific type of radial basis functions, capablity of estimating daily precipitation on a regional scale. This is done with the software package SURFER, Version 6 (Golden Software, Inc. 1995). Beforehand, spatial correlation and anisotropy within the data were analysed with VARIOWIN 2.2 (Pannatier 1996). A geometric anisotropy along the NE-SW axes was identified. Anisotropy was reflected in the interpolation model by anisotropy ratios that were associated with the ranges of the directional variogram models. The performance of the estimation was assessed by traditional statistical methods. In order to highlight possible consequences of errors of decision making, a typecasting of errors was carried out by simplified decision rules with relevance to environmental objectives.**
KEYWORDS: **multiquadric function, classification of errors, decision making**

Contents

---

1 Introduction

In environmental sciences the description of the spatial variability of different parameters has been necessary for various issues. To mention some, physical and ecological process models often require a spatial pattern of some of the input variables. Furthermore, decisions related to the assessment of contamination and the need for remedial actions are based on the spatial pattern of the relevant contaminants. However, most of these parameters can only be measured at particular spots (e.g. at weather stations, in monitoring wells). To receive a spatial distribution interpolation of data from irregular networks has to be applied frequently.

Spatial interpolation techniques are many and various, but when choosing a method the type of surface being interpolated, particularly its smoothness, must be considered (Robeson 1997). For interpolating the spatial variation of soil and hydrological attributes, there seems to be a tendency in favour of kriging and distance-weighting methods. Radial Basis Functions such as thin-plate splines are supposed to be as flexible and as applicable as kriging estimators. Although the algorithm is extremely time-consuming for large data sets, the method was successfully used to interpolate digital elevation models (Desmet 1997) and global-scale topography (Robeson 1997).

However, interpolation always introduces spatially varying errors that propagate through successive models and decisions. For example, Phillips and Marks (1996) showed how interpolation errors of temperature, humidity and wind speed propagated in a spatially distributed physical evapotranspiration model. Myers (1997) emphasised how interpolation errors affected decisions concerning remedial actions. In order to assess the reliability of model outputs and decisions, the uncertainty of interpolations has to be examined.

In what follows investigation of whether multiquadric functions, which belong to the group of the radial basis functions, are capable of interpolating daily precipitation data throughout Switzerland. The study was done within the framework of the Spatial Interpolation Comparison 1997 (SIC97) which means that data from 100 measurement sites were interpolated in order to estimate precipitation at another 367 measurement locations. After that the observed precipitation amounts at those 367 sites were compared to the estimates so that the performance of the interpolation procedures could be assessed.

The precipitation data have been related to the Chernobyl Nuclear Power Plan accident and to the radioactive plume that crossed Europe in May 1986. Since radioactive deposition on the ground mainly depends on rainfall, rainfall fields can help to identify possible contaminated areas and associated risks. In order to highlight consequences of

interpolation errors on decision making, simplified decision rules were used to classify observed and estimated data. A comparison of the two classifications showed misclassifications and therefore false decisions.

2 Methods

2.1 Interpolation method

Interpolation of the 100 initial data points was done by the multiquadric function, which belongs to the group of the radial basis functions (RBF). These are a diverse group of exact interpolation methods that differ according to the chosen basis function. They produce a surface that passes as close as possible through the data points and still maintains a certain degree of smoothness. The multiquadric function is given by the following equation:

$$B_i(x,y) = \sqrt{d_i(x,y)^2 + R^2} \quad (1)$$

where $B_i(x,y)$ is the radial function of the distance $d_i(x,y)$, $d_i(x,y)$ is the anisotropically rescaled, relative distance from the data point (x_i, y_i) to the interpolation grid node (x, y), and R^2 is a smoothing parameter.

During interpolation, the basis functions $B_i(x, y)$ for n data points are optimally weighted at every grid node by coefficients that are determined by solving a linear equation system.

In the software package SURFER® V. 6.0 (Golden Software, Inc. 1995) anisotropy can be considered and a wide range of smoothing parameter R^2 can be chosen. In order to examine spatial anisotropy the data were analysed in VARIOWIN 2.2 (Pannatier 1996). Experimental variograms were calculated omnidirectional and in the four cardinal directions. All the variograms were fitted by a spherical model with the parameters listed in Table 1. The ranges of the variogram model changed considerably depending on the direction while the sill remained constant. Such anisotropy type is referred to as a geometric anisotropy.

Once anisotropic structures are identified, they should be included in the interpolation model. Since the ratios of the ranges of the directional variograms yielded anisotropy-ratios up to 4 along the NE-SW axis, three approaches - MQ1, MQ2 and MQ4 - were distinguished by anisotropy-ratios in 45° direction of 1 (no anisotropy), 2 and 4, respectively (Table 2). Additionally, the radii of the search ellipse were adapted.

Table 1 Parameters of the variogram fitting in VARIOWIN 2.2.

Direction	Variogram Model	Nugget	Sill	Range	Goodness of fit
omnidirectional	Spherical	280	14 000	76 000	0.0410
0° (N-S)	Spherical	2660	14 000	64 000	0.2120
45° (NE-SW)	Spherical	280	14 000	210 000	0.0249
90° (E-W)	Spherical	1680	14 000	109 800	0.1314
135° (SE-NW)	Spherical	1260	14 000	58 000	0.2367

Table 2 Parameters for the anisotropy and the search ellipse used in all interpolations.								
#	Anisotropy-Ratio	Anisotropy-Angle	Search-Type	Max Data	Min Data	Search-Radius 1	Search-Radius 2	Search-Angle
MQ1	1	-	Simple	24	5	210 000	58 000	45°
MQ2	2	45°	Simple	24	5	210 000	58 000	45°
MQ4	4	45°	Simple	24	5	210 000	58 000	45°

A more crucial parameter is the smoothing parameter R^2. Unfortunately, there is no universally accepted method for computing its optimal magnitude. The program SURFER provides a figure for R^2 which is between the average sample spacing and one-half the average sample spacing. Since it may influence the results seriously, interpolations in which R^2 ranged from 0 to 5.0E09 were carried out and the resulting contour lines were compared by eye. Scenarios where considerable changes occurred were then examined in more detail by cross validation. The cross validation results were statistically assessed (see below), and the amount for R^2 that yielded the best results was chosen for each MQ-approach to estimate the data at the 367 additional measurement sites.

2.2 Methods for assessing performance of an interpolation model

By subtracting an observed value from an estimate at a given location magnitude, sign and classification of the estimation error are determined. Observed and estimated values can be obtained in two different ways: First, by cross validation, which means that each sample location is successively removed from the original data set and that its value is estimated from the remaining sample locations. At additional measurement sites (that were not involved in the interpolation process), however, the observed amounts can be compared directly to the estimates from the interpolation.

Since no interpolation model is likely to perform best for all locations, statistical criteria against which the overall performance is measured are needed. For example, the mean bias error (MBE), which indicates a bias in estimation when it is nonzero, is calculated with equation 2. Furthermore, the summary statistics of the root mean squared error (RMSE), the mean absolute error (MAE) and the mean relative error (MRE) given by the equations 3, 4 and 5, respectively, incorporate bias and spread of the errors.

Mean Bias Error: $MBE = \frac{1}{n}\sum_{i=1}^{n}(\hat{P}_i - P_i)$ (2)

Root Mean Squared Error: $RMSE = \sqrt{\frac{1}{n}\sum_{i=1}^{n}(\hat{P}_i - P_i)^2}$ (3)

Mean Absolute Error: $MAE = \frac{1}{n}\sum_{i=1}^{n}\left|\hat{P}_i - P_i\right|$ (4)

Mean Relative Error: $MRE = \frac{1}{n}\sum_{i=1}^{n}\left|\frac{\hat{P}_i - P_i}{P_i}\right|$ (5)

where: n number of rain gauge, P_i observed rainfall at rain gauge i, and $\hat{P}_i$ estimated rainfall at rain gauge i.

Since good estimations of rainfall fields can help to identify areas possibly contaminated by (radioactive) deposition, the performance of estimation was also judged with regard to risk analysis and decision making. Thus, it was examined how well the ten highest and the ten lowest rainfall data of the whole data set (467 data) were estimated by the methods applied. Both, the precision of the spatial location and the accuracy of the precipitation amounts were considered.

In addition, an approach of typecasting of errors following Myers (1991, 1997) was carried out, which allows us to compare different estimators based on environmental objectives. Decisions, whether certain measures will be introduced or not, are often related to thresholds or action levels. Therefore, observed and estimated data were classified with simplified decision rules. For example, in the case of radioactive fallout people could be warned to harvest garden fruits and vegetables and to put cows out to pasture, if precipitation and thus the contamination of an area exceeded a given threshold. 1. "Immediate measures", such as prohibition of putting livestock out to pasture along with a sophisticated monitoring program in dairies could be introduced if precipitation was even above a certain threshold 2. For a virtual case study, it was assumed that areas where rainfall was below 2 mm had not been affected by fallout so that no measures had to be introduced. On the other hand, areas which had received 40 mm daily rainfall or more should have been chosen for "immediate measures". In such a decision process interpolation errors propagate and might cause misclassifications and, therefore, false decisions. Figure 1 shows a misclassification ellipse and the typecasting of errors for decisions that are related to two threshold concentrations indicating different action levels. If the estimated concentration exceeds the threshold concentration although the actual value falls below that threshold, an error of type I or false positive results. An error of type II (false negative) appears when the estimated value is below the threshold concentration, but the true concentration is above.

This approach is highly effective in conjunction with cross validation in order to find optimal interpolation parameters for performance-based goals (e.g., Myers 1997). In what follows, this procedure was also used to compare observed and estimated precipitation at the 367 additional measurement sites.

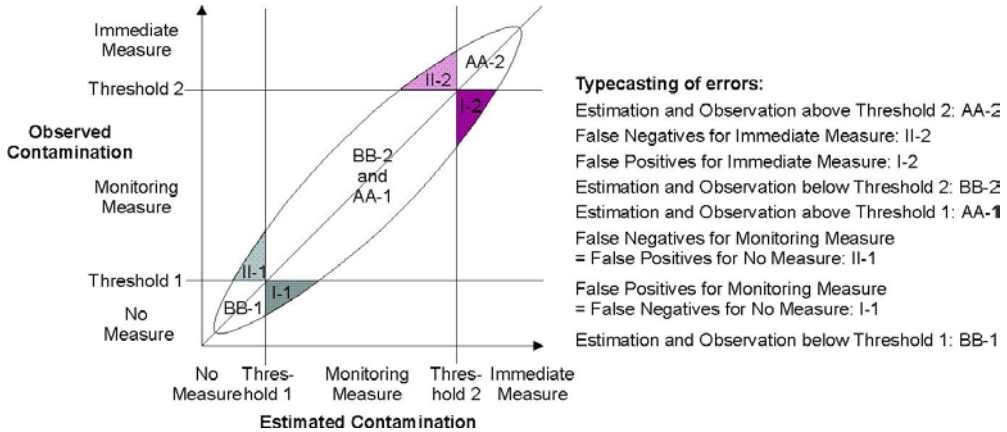

Figure 1 Misclassification ellipse for two thresholds (derived from Rendu 1980) and typecasting of errors (derived from Myers 1991).

3 Results and discussion

3.1 Assessment and optimization of interpolation by cross-validation

Since associated parameters of an interpolation method like the smoothing parameter R^2 in the multi-quadric function may influence the results seriously, these parameters should be optimized before the final estimation is done. Therefore, interpolations with R^2 ranging from 0 up to 5.0E09 were carried out and the resulting contour lines were compared by eye. Interpolation results remained rather constant from $R^2 = 0$ to $R^2 = 500\ 000$, but altered from $R^2 > 500\ 000$ onwards in all three cases (MQ1, MQ2, and MQ4). Therefore cross validation was performed considering the following values for R^2: 0, 4.75E06, 1.37E07, and 4.96E07. The last three figures were suggested by the software package as reasonable values for the case MQ4, MQ2, and MQ1, respectively.

The statistics of the estimates and the residuals from the cross-validation processes are summarized in Table 3 and Table 4. They revealed that minimum and maximum precipitation amounts were over- or underestimated, respectively, and that the standard deviation of the estimates was narrower than that of the observed data (Table 3). The higher the R^2, the closer the maximum values and the standard deviations were to the observed ones. However, the statistics of the residuals (Table 4) showed that the residuals increased when R^2 was enlarged and so did the RMSE and the MAE. Only the MRE behaved contrarily. The nonzero means indicated a bias in the estimations.

Table 3 Statistics and classification errors of the observed precipitation [1/10th mm] and the estimates from the cross validation procedures at 100 measurement sites.

#	R^2	min	max	mean	median	standard-deviation	BB-1	I-1	II-1	AA-2	I-2	II-2
observed	-	10	585	180.2	141	116.7	4	-	-	4	-	-
MQ1	0	15	454	182.0	142	98.0	0	4	1	0	1	4
MQ1	4 750 000	16	465	182.3	142	101.2	0	4	1	0	1	4
MQ1	13 700 000	16	471	182.4	139	103.1	1	3	1	0	1	4
MQ1	49 600 000	14	480	182.5	137	106.6	1	3	1	0	1	4
MQ2	0	11	444	181.7	146	100.9	0	4	1	0	1	4
MQ2	4 750 000	12	457	181.9	139	104.1	0	4	1	0	3	4
MQ2	13 700 000	13	464	182.0	140	106.0	0	4	1	0	3	4
MQ2	49 600 000	16	475	181.7	138	109.4	0	4	1	0	3	4
MQ4	0	14	422	181.1	147	101.5	0	4	1	0	4	4
MQ4	4 750 000	15	438	181.4	141	105.5	0	4	1	0	4	4
MQ4	13 700 000	15	457	181.5	143	108.1	0	4	1	0	4	4
MQ4	49 600 000	12	501	181.1	143	113.8	0	4	2	0	4	4

Table 4 Statistics of the residuals from the cross validation procedures.							
#	R^2	min	max	MBE	RMSE	MAE	MRE [-]
MQ1	0	-307	165	2.9	69.4	46.3	0.48
MQ1	4 750 000	-305	174	2.1	69.8	46.4	0.47
MQ1	13 700 000	-304	182	2.2	70.3	46.7	0.46
MQ1	49 600 000	-300	199	2.3	72.1	48.2	0.46
MQ2	0	-268	149	1.6	63.6	43.8	0.44
MQ2	4 750 000	-267	155	1.8	64.6	43.8	0.42
MQ2	13 700 000	-266	158	1.8	65.6	44.2	0.41
MQ2	49 600 000	-271	163	1.6	68.4	45.7	0.41
MQ4	0	-241	143	1.0	59.5	42.4	0.41
MQ4	4 750 000	-242	160	1.3	62.1	43.3	0.40
MQ4	13 700 000	-243	179	1.3	64.8	44.9	0.40
MQ4	49 600 000	-281	223	0.9	72.6	50.4	0.44

The increasing anisotropy ratios in the approaches MQ2 and MQ4 yielded lower minimum and maximum errors, RMSE, and MAE than MQ1. None of the approaches was capable of estimating an adequate amount at the sites where precipitation fell below threshold 1 or exceeded threshold 2 (Table 3). Consequently, classification errors of type I and II occurred. Although the approach MQ4 yielded the lowest amounts for RMSE and MAE in comparison to MQ2 and MQ1, it caused more misclassifications, particularly at the second threshold. This demonstrates that certain measures for performance highlight different aspects so that a single measure is not sufficient. To summarize, it seemed reasonable to apply each of the approaches (MQ1, MQ2, and MQ4) with a smoothing parameter of $R^2 = 0$ to estimate precipitation at the 367 additional locations.

3.2 Comparison between estimated and actual precipitation at additional measurement sites

3.2.1 Assessing performance by statistical criteria

Contour maps of the rainfall throughout Switzerland on 8th May 1986 were drawn from the three interpolation approaches MQ1, MQ2 and MQ4 with the parameters summarized in Table 2, with $R^2 = 0$, and based on 100 observed precipitation data (Figure 2). In all cases precipitation ranged from 0 mm in the east to 50 mm in the south-west. The higher ratio of anisotropy in MQ4 caused rainfall fields to be more extensive along the NE-SW axis and smaller in SE-NW direction than in the cases MQ2 and MQ1.

These three interpolation approaches were also used to estimate precipitation at another 367 sites. An estimator that performs well yields a distribution close to the original sample distribution. Statistics of the observed and estimated precipitation at these additional measurement sites are shown in Table 5. The estimated minimum precipitation generally exceeded the observed value of 0 mm. The observed maximum precipitation of 51.7 mm was underestimated by all approaches. The mean of the MQ1 and MQ2 estimates stayed below the observed mean while the mean produced by MQ4 matched accurately. In all approaches the median of the estimated values was higher than the observed one. Standard deviations were narrower in the estimated values than in the observed, which is a typical effect owing to smoothing inherent in the interpolation

procedure.

Table 5 Statistics of the observed and the estimated precipitation [1/10th mm] at the 367 additional measurement sites.

Statistics	min	max	mean	median	standard deviation
observed	0	517	185.4	162	111.2
MQ1, $R^2 = 0$	14	484	181.8	163	95.8
MQ2, $R^2 = 0$	17	476	183.4	168	98.9
MQ4, $R^2 = 0$	19	491	185.1	165	101.4

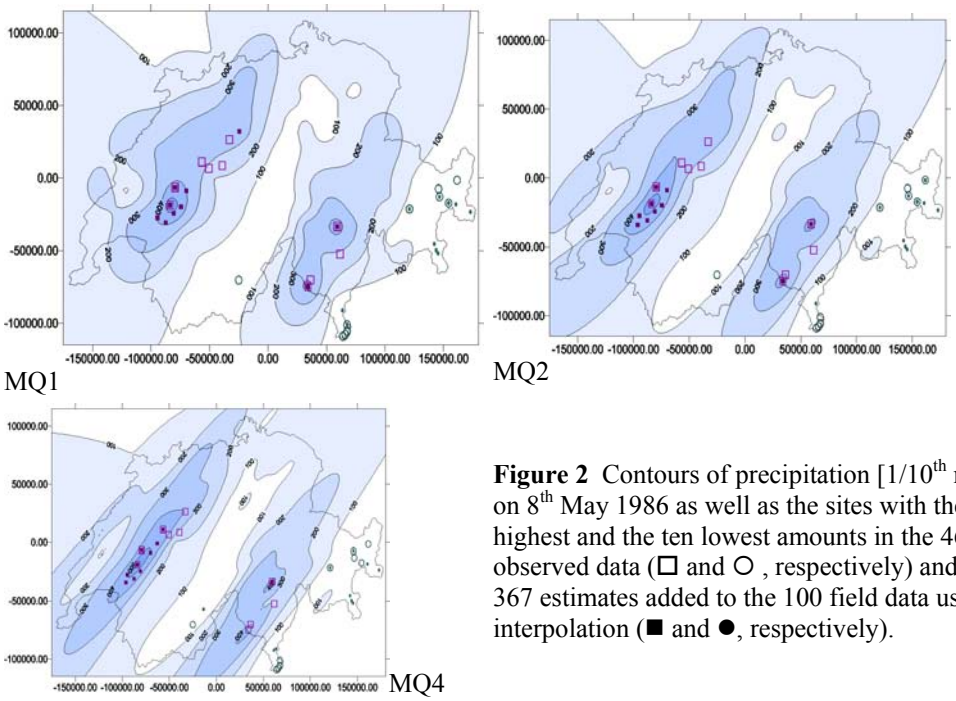

Figure 2 Contours of precipitation [1/10th mm] on 8th May 1986 as well as the sites with the ten highest and the ten lowest amounts in the 467 observed data (□ and ○ , respectively) and in the 367 estimates added to the 100 field data used for interpolation (■ and ●, respectively).

Scatter plots of observed versus estimated precipitation (shown in the left side of Figure 3) enable us to investigate conditional bias in the interpolation models. A perfect estimation would result in a 45° line where actual and estimated values match exactly, but in practice a cloud of points appears instead. Increasing anisotropy ratios in the interpolation models resulted in a slightly narrower distribution along the 45° line. However, still few, but high outliers also remained in case MQ4.

The right side of Figure 3 shows residuals as a function of the observed values. This is another visual method for investigating conditional bias or correlation of errors. In unconditional unbiased estimations, the errors should plot both above and below the horizontal zero line in roughly equal magnitude. For the three interpolation approaches applied here low observed precipitation tended to be slightly overestimated, whereas the estimates of the highest precipitation were far too low. This was a result of the smoothing effect inherent in the interpolation models. However, the overestimation of low precipitation depths slightly increased, the higher the anisotropy ratio in the interpolation model was. On the contrary, the magnitude of residuals at high observed precipitation,

slightly decreased and generally the spread of errors also declined. On the whole, estimation errors tended to correlate with the observed precipitation in all approaches.

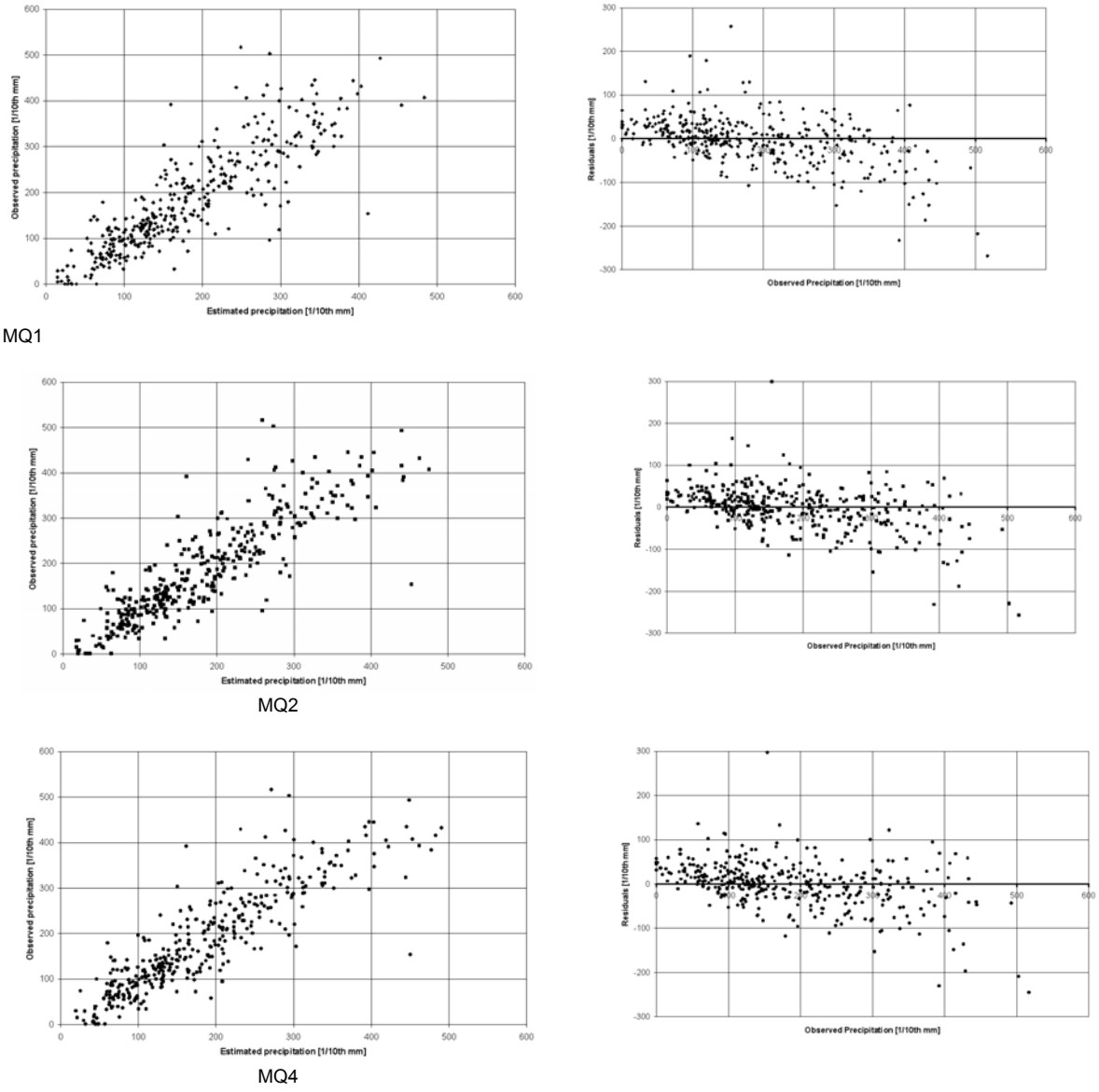

Figure 3 Scatter plots with 367 precipitation data [1/10th mm].
Left: Estimated versus observed precipitation.
Right: Observed precipitation versus residuals (estimation - observation).

Quite a number of residuals amounted up to +/- 10 mm. Considering that the mean observed precipitation was about 18 mm, such estimation errors are rather high. While only one positive error of more than 20 mm occurred, several negative residuals of the same magnitude appeared especially where the observed precipitation exceeded 35 mm.

Figure 4 shows how the residuals were distributed in space. In areas where the interpolation models were supported by evenly scattered measurement sites and in areas where rainfall altered continuously in space, the estimation errors were low. This could

be found in the northern part of the investigation region. However, all of the three approaches failed to predict precipitation that changed rapidly in space. For example, the location where the highest positive error of about 30 mm appeared was surrounded by sites where much higher precipitation was observed so that this local minimum was not estimated well.

High over- and underestimates showed a clustered pattern. These clusters mainly occurred in areas where the interpolation was not or was only sparsely supported by data points. Areas that had received high precipitation were not identified when none of the data from that cluster was included in the interpolation process. On the other hand, data with very high precipitation amounts partly caused considerable overestimation in their surroundings.

The overall performance can be assessed by MBE, RMSE, MAE and MRE (Table 6). The MBE were negatively biased which was mainly due to the large negative estimation errors. MBE decreased in MQ4 as a result of a few higher overestimates at low precipitation values in comparison to MQ1 and MQ2. RMSE as well as MAE decreased in relation to the anisotropy ratio in MQ1, MQ2 and MQ4. In general, the amounts of RMSE (5.3 to 5.6 mm) were higher than the values of MAE (3.7 to 3.9 mm) because the RMSE is more sensitive to high residuals. MQ2, followed by MQ4 and MQ1, performed best, but a MRE of 37 % still remained.

Owing to a better consideration of the anisotropy detected by spatial data analysis, MQ2 and MQ4 yielded better results than MQ1. It has to be concluded that pre-modelling is an approach to improving interpolation models. However, the overall performance remained rather poor.

Table 6 Summary statistics of the observed and estimated precipitation data at the 367 additional measurement sites.

#	MBE [1/10th mm]	RMSE [1/10th mm]	MAE [1/10th mm]	MRE [-] *
MQ1, $R^2 = 0$	-3.6	55.7	38.8	0.38
MQ2, $R^2 = 0$	-1.9	53.1	36.7	0.37
MQ4, $R^2 = 0$	-0.3	53.3	37.3	0.45

(*: At five measurement sites no precipitation was observed. Since this caused a division by zero, these sites were neglected in MRE.)

3.2.2 Performance of estimating the ten highest and the ten lowest precipitation amounts

In Figure 2 squares and circles indicate the locations of the ten highest and the ten lowest precipitation amounts, respectively. The sites related to the estimated values are drawn by filled symbols and include the 100 data that were used for the interpolation. These 100 field data included three out of the ten highest amounts in the whole data set and one out of the ten lowest data.

The highest estimates were mainly located in the neighbourhood of the precipitation site where 58.5 mm was observed, while the lowest estimates almost entirely appeared in the eastern part of Switzerland. Table 7 summarises the number of matched locations, which are locations where both, actual data and estimates, belonged to the ten highest and the ten lowest amounts in the 467 data. Additionally the ranges of the precipitation amounts are given. The ranges of the highest and lowest estimates were of the same order of magnitude in the observations and in the three interpolation models. There was a shift towards higher precipitation from MQ1 to MQ4 according to the anisotropy ratios. However, none of the interpolation models succeeded in identifying the clusters of high

precipitation in the middle of the investigation area since no data from there had supported the interpolation.

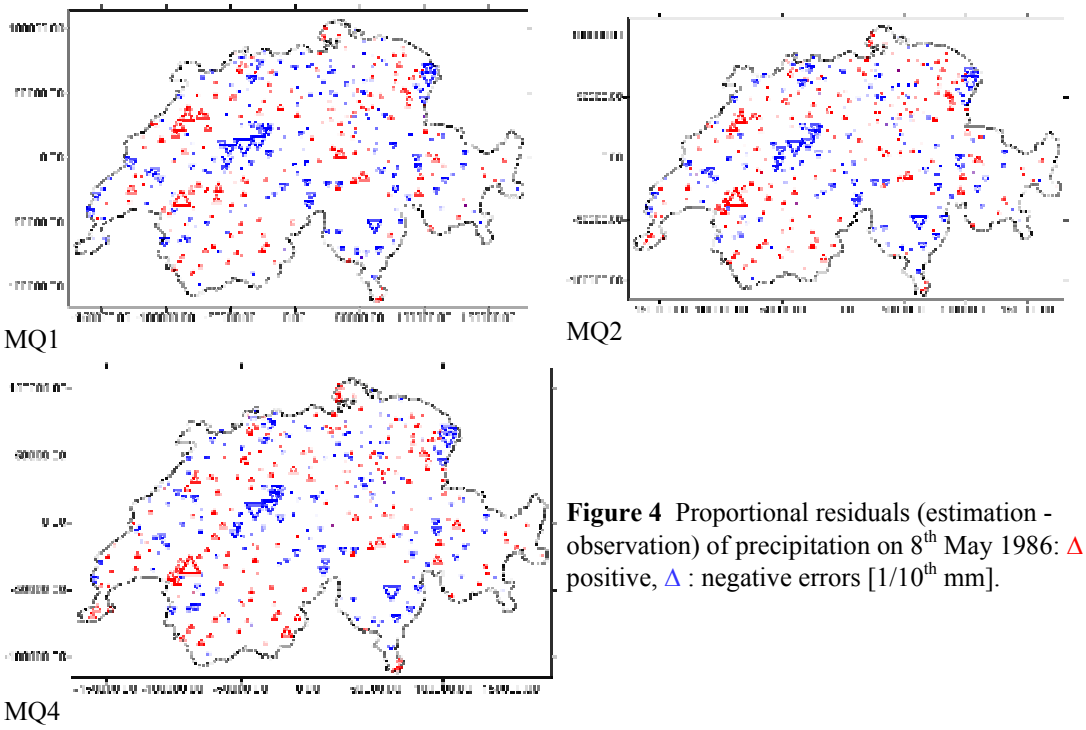

Figure 4 Proportional residuals (estimation - observation) of precipitation on 8th May 1986: Δ : positive, Δ : negative errors [1/10th mm].

Table 7 The number of matched locations (both, actual data and estimates, belong to the ten highest and the ten lowest data in the 467 data) and ranges of the ten highest and the ten lowest precipitation amounts.

	10 lowest precipitation data		10 highest precipitation data	
	matched locations	precipitation [1/10th mm]	matched locations	precipitation [1/10th mm]
observed	10	0 .. 10	10	434 .. 585
MQ1	4	10 .. 24	4	398 .. 585
MQ2	4	10 .. 20	4	440 .. 585
MQ4	2	10 .. 31	4	446 .. 585

3.2.3 Performance of estimating precipitation amounts $P \geq 40$ mm and $P \leq 2$ mm

As outlined above data that exceeded P = 40 mm were supposed to indicate a need for "immediate measures", whereas areas where precipitation fell below P = 2 mm would receive no measure at all (see Figure 1). With these simplified decision rules observed and estimated precipitation data were classified into three groups. Owing to interpolation errors different numbers and types of true and false decisions occurred (Table 8). Their spatial location is shown in Figure 5. The total number of sites where precipitation fell below threshold 1 and exceeded threshold 2 was lower in the estimated sets than in the observed one due to smoothing through the interpolation processes. While in case MQ1 both classes ($P \leq 2$ mm, $P \geq 40$ mm) were equally filled, there was a shift towards fewer numbers below threshold 1 and more above threshold 2 in MQ4.

Table 8 The number and types of true and false decisions at the two thresholds.						
	Threshold 1: P ≤ 2mm			Threshold 2: P ≥ 40 mm		
	Type I	Type II	BB	Type I	Type II	AA
Observed	-	-	18	-	-	22
MQ1, $R^2 = 0$	11	1	7	2	15	7
MQ2, $R^2 = 0$	10	2	8	4	12	10
MQ4, $R^2 = 0$	14	1	4	7	11	11

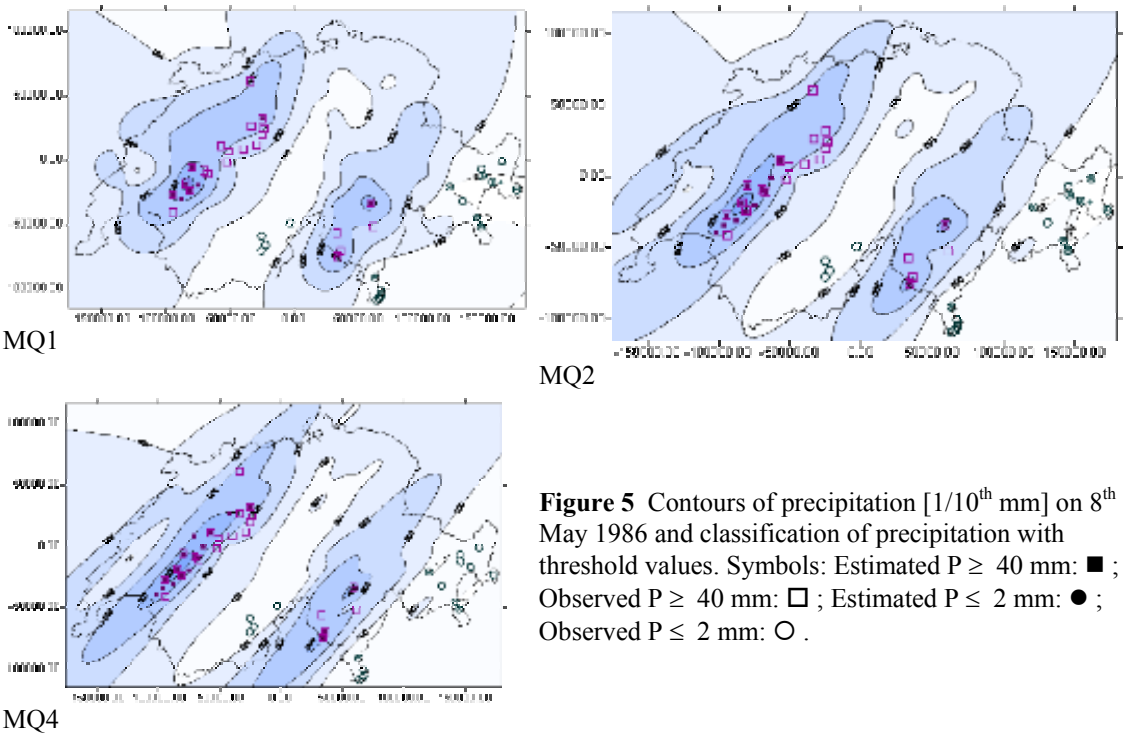

MQ1 MQ2 MQ4

Figure 5 Contours of precipitation [1/10th mm] on 8th May 1986 and classification of precipitation with threshold values. Symbols: Estimated P ≥ 40 mm: ■ ; Observed P ≥ 40 mm: □ ; Estimated P ≤ 2 mm: ● ; Observed P ≤ 2 mm: ○ .

Moreover, an increasing anisotropy ratio caused more false positives (Error Type I) at both thresholds and less false negatives (Error Type II) at the second threshold. At threshold 1 right decision (BB) decreased, but increased at threshold 2 (AA). This approach thus shows the bias and smoothing within the estimators in a simple manner. Nevertheless, this technique functions well to evaluate interpolation results in the framework of decision making. The interpolation model that succeeded in providing the most accurate decisions would be chosen in practice.

4 Conclusions

Altogether, the approach MQ2 provided the best estimates of precipitation at the 367 additional measurement sites. Owing to the better consideration of anisotropy, both MQ2 and MQ4 yielded better results than MQ1. Therefore, it has to be concluded that spatial data analysis and consideration of anisotropy can improve interpolation results with the multi-quadric function. However, the overall performance is poor. The multi-quadric function was rarely capable of estimating precipitation that changed rapidly in space as it occurs in daily rainfall fields in mountainous regions. Particularly the performance of estimating high precipitation amounts was rather poor. The smoothing effect inherent in the interpolation procedure caused a biased estimation in which low precipitation data were overestimated and high precipitation data were clearly underestimated. In the case of a nuclear accident rapid and reliable estimations are needed especially to recognize areas that have received high precipitation. Since this target is badly met by the approaches shown in this paper, it has to be concluded that they should not be applied to estimate heterogeneous rainfall fields.

Since residuals from the cross validation processes also revealed the weak points of interpolations with the multi-quadric function, this technique can be used to optimize the interpolation model and to provide some measure for the uncertainty of the interpolation. For example, the mean relative error could be imposed on the estimates. However, it should be noted that the RMSE, the MAE and the MRE calculated from the residuals from the cross validation processes were higher than the corresponding amounts from the residuals at the 367 additional measurement sites. That means that the uncertainty of the interpolation tends to be overestimated when it is solely derived from cross validation results. Nevertheless, this procedure can be used for the optimization of interpolation with regard to the choice of the basis function, the parameter R^2, anisotropy and search parameters. Regions where high residuals and misclassifications still remain should be suggested for additional field sampling.

References

Desmet, P. J. J. (1997) Effects of Interpolation Errors on the Analysis of DEMs, *Earth Surface Processes and Landforms*, 22, 563-580.

Golden Software, Inc. (1995) *SURFER® for Windows Version 6.0 User's Guide*. Colorado: Golden Software, Inc.

Myers, J. C. (1991) Geostatistical Error Management for Site Assessment (GEM). In: Proceedings of HAZMAT West 1991, Long Beach.

Myers, J. C. (1997) Geostatistical Error Management - Quantifying Uncertainty for Environmental Sampling and Mapping. New York: VNR.

Pannatier, Y. (1996) *Variowin*: *Software for Spatial Data Analysis in 2D*. New York: Springer.

Phillips, D. L. and D. G. Marks (1996) Spatial uncertainty analysis: propagation of interpolation errors in spatially distributed models, *Ecological Modelling*, 91, 213-229.

Rendu, J-M. (1980) *Optimizations of Sampling Policies: A Geostatistical Approach*. Tokyo: MMIJ-AIME.

Robeson, S. M. (1997) Spherical Methods for Spatial Interpolation: Review and Evaluation, *Cartography and Geographic Information Systems*, 24, 3-20.

JGIDA vol. 2, no. 2
JGIDA Home